



---

## Figures and figure supplements

Recreating the synthesis of starch granules in yeast

**Barbara Pfister et al**

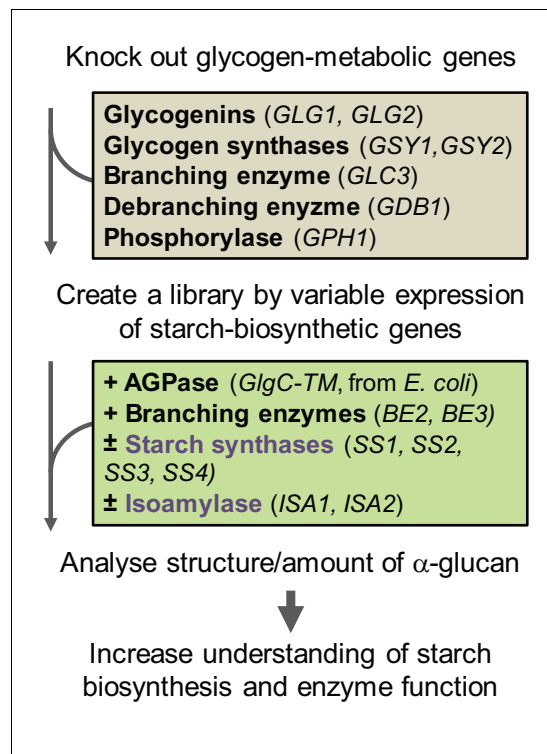


**Figure 1.** Workflow of the *S.cerevisiae* system. The yeast's endogenous glycogen-metabolic pathway (grey box) was removed and varying components of the starch-biosynthetic pathway from Arabidopsis (green box) was introduced. The deregulated mutant of ADPglucose pyrophosphorylase (AGPase) from *E. coli* was used for the supply of ADPglucose. For details of the constructs see **Figure 1—figure supplement 1**. DOI: [10.7554/eLife.15552.003](https://doi.org/10.7554/eLife.15552.003)

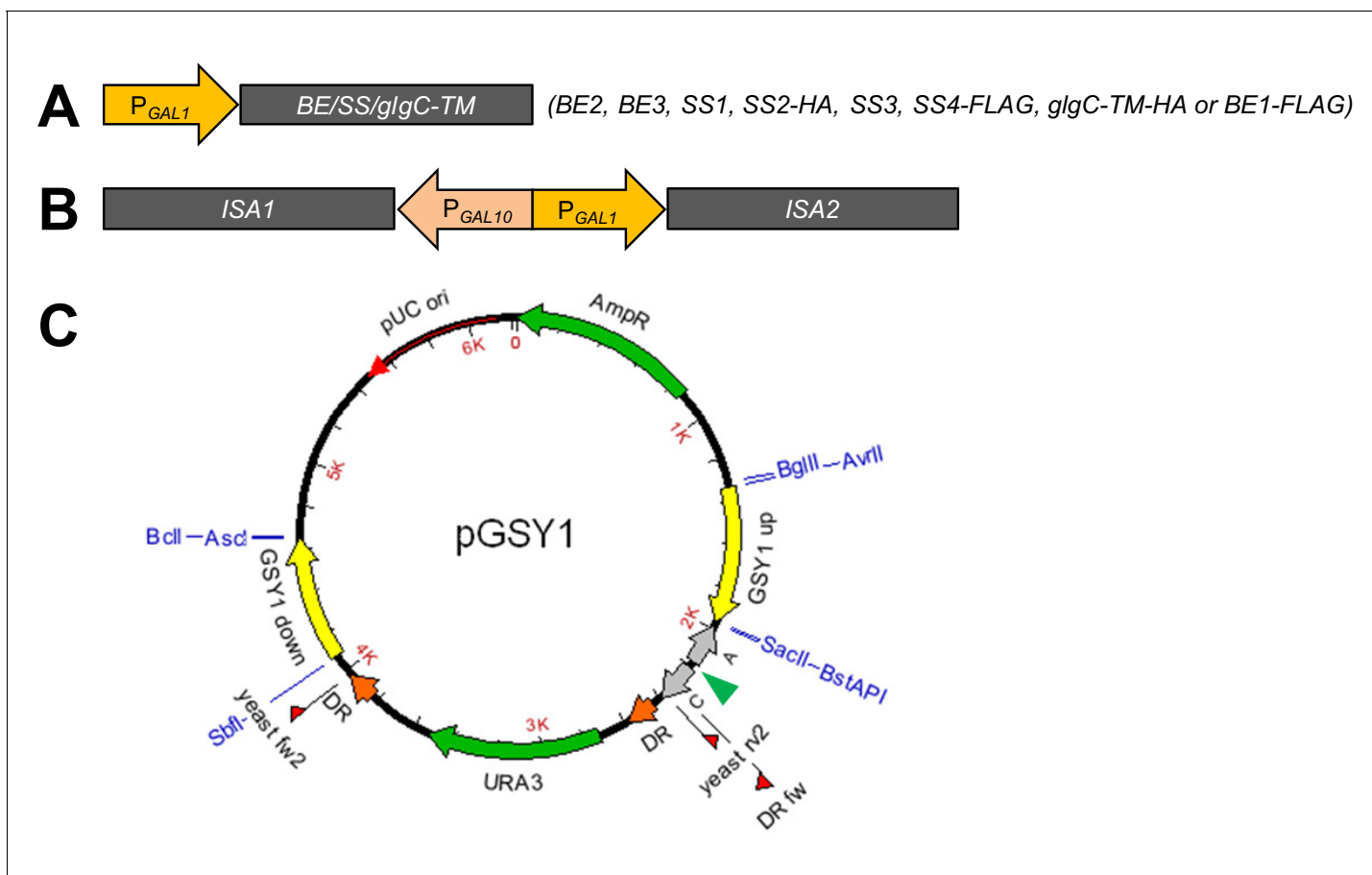


**Figure 1—figure supplement 1.** Constructs for heterologous gene expression and/or deletion of endogenous genes. (A) Expression constructs contain the coding sequence (less chloroplast transit peptide) of Arabidopsis branching enzymes BE2 or BE3, the putative branching enzyme BE1, starch synthases SS1 to SS4 or bacterial *glgC*-TM (encoding an allosterically insensitive ADPglucose pyrophosphorylase) fused to galactose-inducible  $P_{GAL1}$  promoters. SS2 is tagged with a C-terminal HA tag and SS4 and BE1 with a C-terminal FLAG tag, as their activities are not observed in zymograms from plant extracts. Similarly, *glgC*-TM carries a C-terminal HA tag. (B) ISA1 and ISA2 were combined within a single construct using the bidirectional  $P_{GAL10}$ - $P_{GAL1}$  promoter. (C) Example of an empty yeast integration vector. The insertion site for the expression construct is indicated with a green arrowhead. The vectors additionally contain terminator sequences (CYC1 [C] and ADH1 [A] terminators, grey arrows), a URA3 gene for selection (flanked by direct repeats [DR] for later marker recycling) and regions homologous to genome sequences of yeast (here GSY1 up or GSY1 down, yellow arrows). The homologous regions target the insert either to glycogen-metabolic genes (replacing the majority of the gene; here the GSY1 gene) or between essential genes (Mikkelsen et al., 2012). Restriction sites used for the creation of the vectors are depicted in blue. Plasmid-based primers for genotyping of transgenic yeast strains are shown as red flags (described in **Supplementary file 1D**).

DOI: [10.7554/eLife.15552.004](https://doi.org/10.7554/eLife.15552.004)

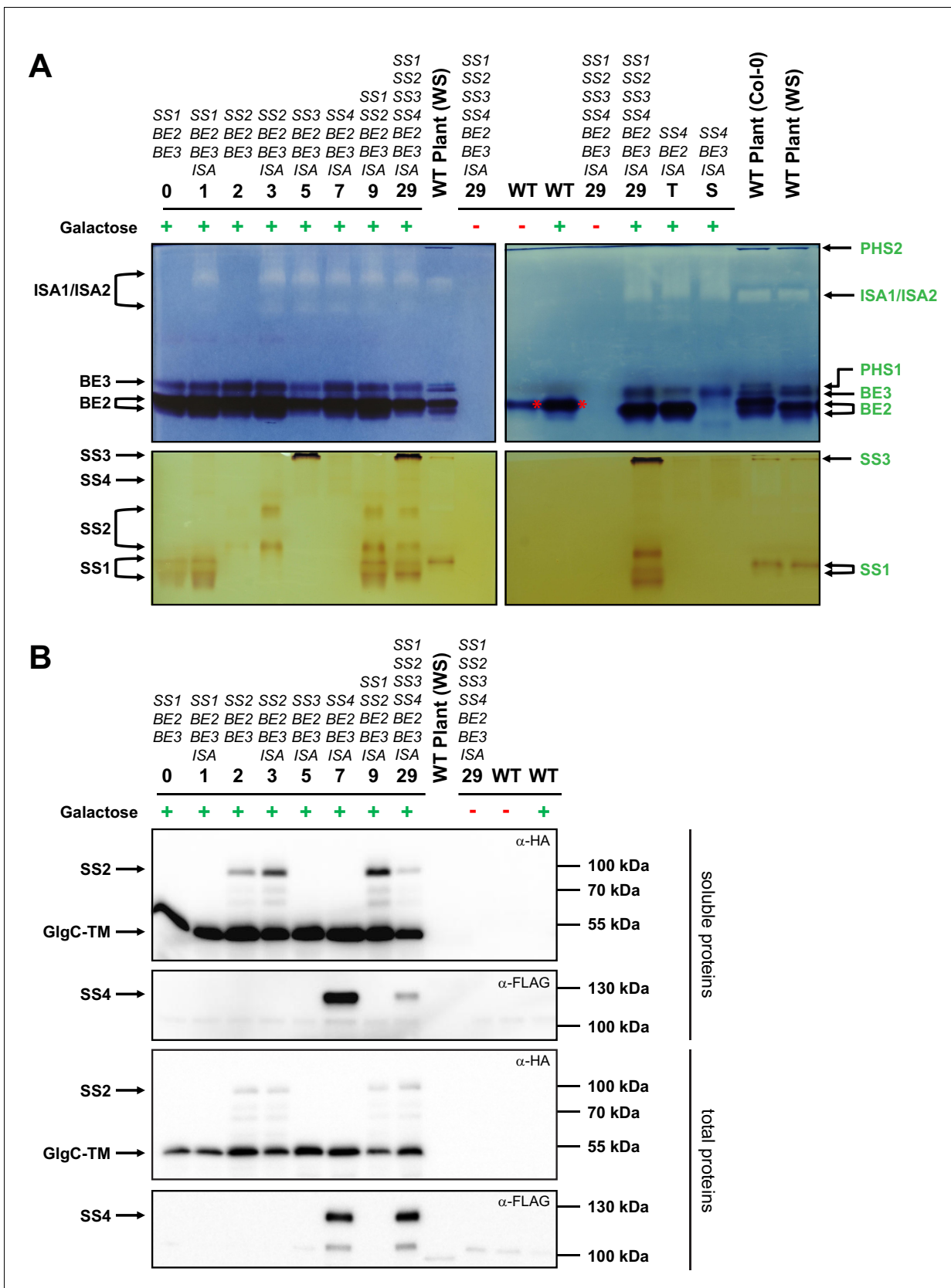


**Figure 2.** Native PAGE and immunoblots of heterologously expressed proteins. Total proteins or native soluble proteins were extracted from yeast lines grown in liquid cultures with complex medium. Native soluble proteins were subjected to native PAGE for detection of enzyme activity (A) and Figure 2 continued on next page

## Figure 2 continued

SDS-PAGE followed by Western blotting (B, upper panels). Total proteins were also subjected to Western blots (B, lower panels). Whether the yeast main cultures contained galactose (+) or glucose (-) is indicated. Arabidopsis genes present in the yeast lines are given above the strain number (see **Supplementary file 1A** for complete genotypes), and all yeast lines except for the wild type (WT) also contain the *glgC-TM* gene. (A) Native PAGE of soluble proteins in glycogen-containing gels that were incubated either with glucose-1-phosphate and phosphorylase (for visualization of branching enzyme and isoamylase activity, top panel) or ADPglucose (for visualization of starch synthase activity, bottom panel). The left- and right-hand panels show separate gels that were processed at the same time. Glucan-modifying activities were revealed by iodine staining. Strains expressing only one branching enzyme (lines T and S) and WT Arabidopsis plant extracts (WS or Col-0 ecotype) are shown for comparison. Enzyme activities in plant extracts, deduced from earlier mutant analyses, are indicated on the right hand side in green (for a representative summary refer to Supplemental Fig. S1 in **Pfister et al. [2014]**). Enzyme activities in yeast extracts, deduced from strain comparisons, are indicated on the left side in black. BE2 migrates as three activities; two very close bands (indicated with the double arrow) and a third slower band that overlaps with BE3 activity (compare strains T and S). SS4 gives a weak but distinct band, as indicated. The branching activity in WT yeast is the endogenous branching enzyme, Glc3p (red asterisk). PHS1, plastidial phosphorylase; PHS2, cytosolic phosphorylase. (B) Immunoblots of yeast soluble protein extracts (upper two panels) and yeast total protein extracts (lower two panels), respectively, after separation by SDS-PAGE. The plant sample is the same soluble protein extract in both cases. SS2, GlgC-TM (both carrying a C-terminal HA tag) and SS4 (carrying a C-terminal FLAG tag) were visualized using  $\alpha$ -HA or  $\alpha$ -FLAG antibodies, as indicated. The expected molecular weights are 83 kDa for SS2-HA, 50 kDa for GlgC-HA and 116 kDa for SS4-FLAG. Soluble and total proteins are shown because each protein's abundance in the soluble extract is influenced by its binding to glucans and the resultant partitioning between the soluble and insoluble fraction. The signal intensities from the soluble proteins should not be compared with those from total proteins as they arise from separate blots. The following figure supplement is available for **Figure 2**:

DOI: [10.7554/eLife.15552.005](https://doi.org/10.7554/eLife.15552.005)

The following source data is available for figure 2:

**Source data 1.** Glucan contents and  $\lambda_{\max}$  values of individual replicates.

DOI: [10.7554/eLife.15552.006](https://doi.org/10.7554/eLife.15552.006)

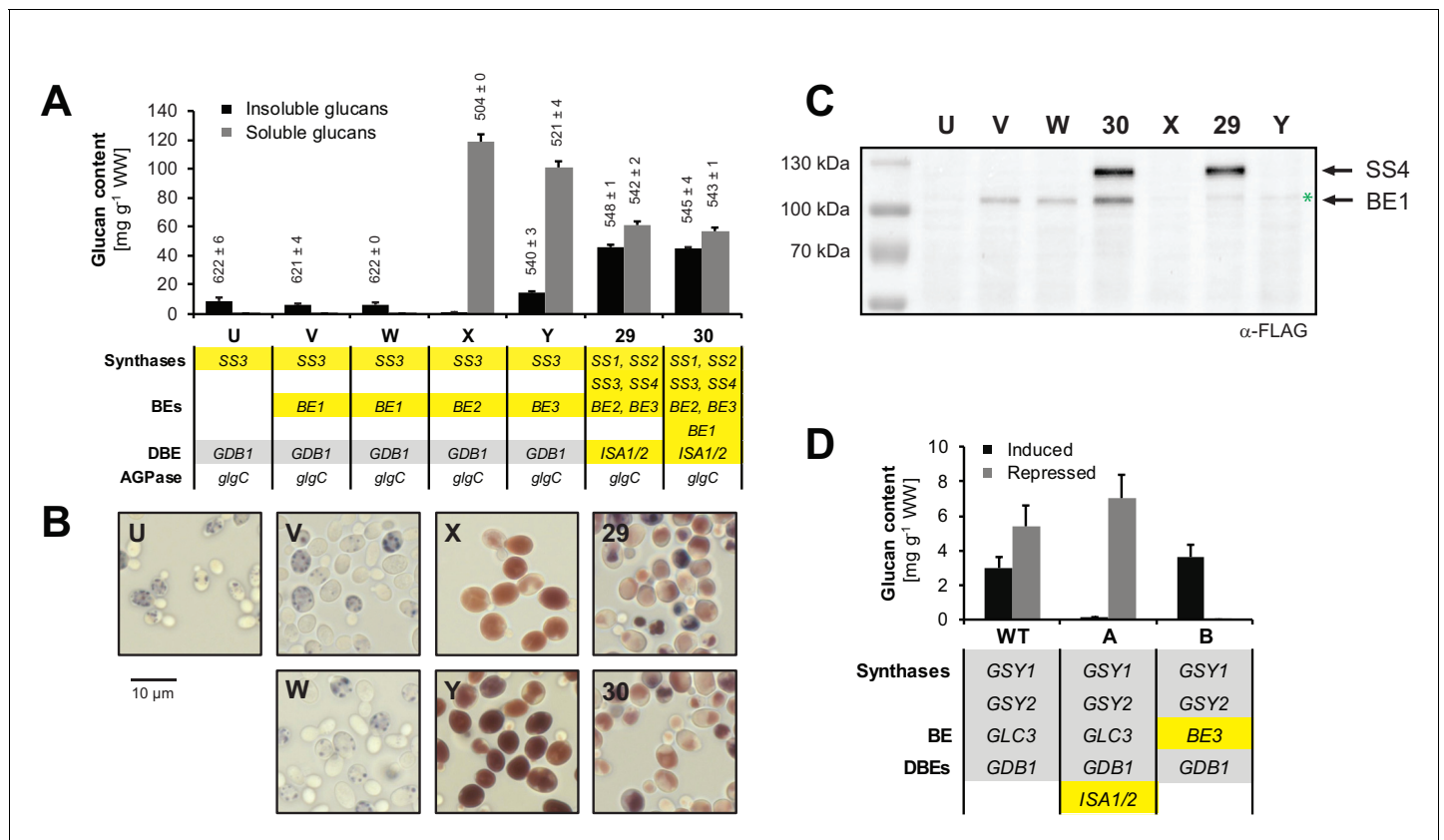


**Figure 2—figure supplement 1.** Enzyme function of ISA1/ISA2, BE1, BE2 and BE3 in yeast. The relevant genotypes are indicated; the Arabidopsis genes are highlighted in yellow and the endogenous yeast genes in grey. The WT and the strains A, B, U to Y also contain the endogenous glycogenin (*GLG1*, *GLG2*) and phosphorylase (*GPH1*) genes. Lines V and W are individual isolates from the same transformation event. Genotypes are listed in **Supplementary file 1A**. (A) Quantification of insoluble (black bars) and methanol-precipitable soluble (grey bars) glucans and their wavelengths of maximum absorption after complexation with iodine ( $\lambda_{max}$ ; values above the bars, in nm). Yeast lines were grown for 6 hr in liquid main cultures with galactose. Values are means  $\pm$  S.D. from 3 replicate cultures for the quantifications (except for strain 30 where  $n = 4$ ) and from 2 replicate cultures for the  $\lambda_{max}$  measurements (except for strain 29 where  $n = 4$ ). Malto-oligosaccharide content in strains U, V, W, X and Y was  $<0.7$  mg g<sup>-1</sup> wet weight (WW) including S.D. Note that the glucans made with BE1 (lines V and W) or in the absence of any BE (line U) have a  $\lambda_{max}$  typical of long linear chains. The glucans from strain 29 (expressing all core amylopectin-biosynthetic genes) were also very similar to those from strain 30 (expressing also BE1) in terms of chain-length distribution, granule morphology and X-ray scattering patterns (not shown; see results section 'Yeast glucans have semi-crystalline properties of starch' for a description of these techniques). WW, wet weight; BE, branching enzyme; DBE, debranching enzyme; AGPase, ADPglucose pyrophosphorylase. (B) Light micrographs (LM) of the indicated yeast lines grown as in A. Cells were stained with iodine. (C) Anti-FLAG immunoblots of yeast total protein extracts from cultures grown as in A. The expected molecular weights are 99 kDa for BE1-FLAG and 116 kDa for SS4-FLAG. The weak band slightly above BE1-FLAG reflects unspecific binding of the antibody (marked by a green asterisk). (D) Yeast carrying *ISA1/ISA2* or *BE3* (replacing the endogenous branching enzyme *GLC3*) under galactose-inducible promoters were first grown in complex medium and then transferred to medium lacking nitrogen to trigger glycogen synthesis. Media contained either galactose (strongly inducing heterologous gene expression; black bars) or glucose (strongly repressing expression, grey bars) as the sugar source. Induction of *ISA1/ISA2* suppressed glucan accumulation (line A). Induction of *BE3* (line B) in an otherwise BE-deficient strain restored glycogen synthesis. Shown are mean values  $\pm$  S.D. of 3 replicate cultures. WW, wet weight; BE, branching enzyme; DBEs, debranching enzymes.

DOI: 10.7554/eLife.15552.007

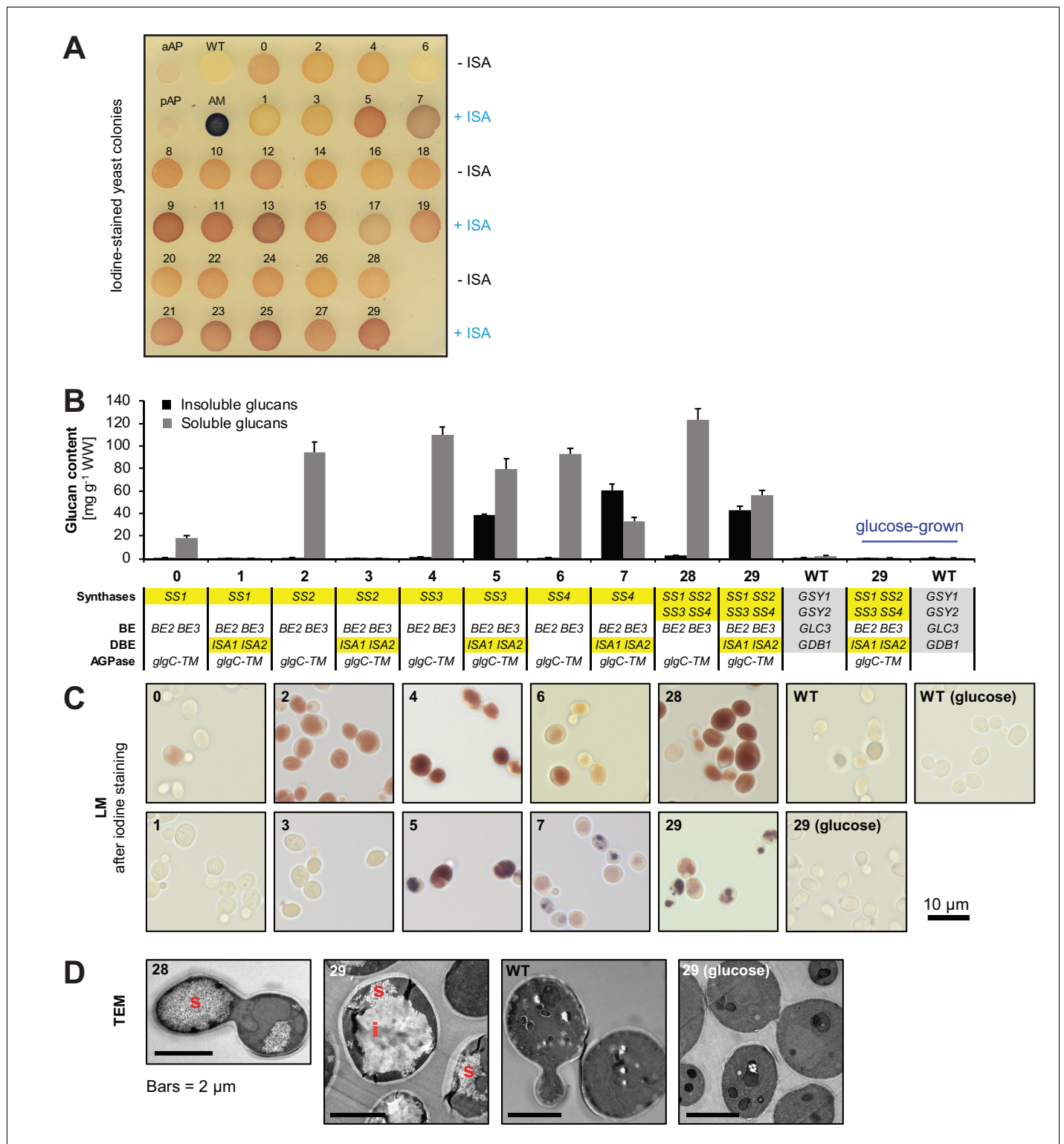


**Figure 3.** Yeast strains synthesize high amounts of glucans. (A) Iodine staining of 30 yeast strains (numbered 0–29) which vary the complement of SS isoforms and ISA1/ISA2 in the glycogen-metabolism free background. Cells were grown for 24 hr on plates with galactose and then stained with iodine vapor. Wild-type (WT) yeast, potato amylose (AM) dissolved in DMSO and native, non-gelatinized plant amylopectins from Arabidopsis (aAP) and potato (pAP) are shown for comparison. Indicative genotypes are given in B and **Figure 3—figure supplement 1**. Full genotypes are listed in **Supplementary file 1A**. (B) Quantification of insoluble (black bars) and methanol-precipitable soluble (grey bars) glucans of yeast lines grown for 6 hr in liquid main cultures with galactose. The genotypes are indicated; the varying SS and ISA1/ISA2 genes are highlighted in yellow and the endogenous **Figure 3 continued on next page**

*Figure 3 continued*

yeast genes in grey. For the glucose-grown cultures in **B-D**, galactose was replaced by glucose to repress heterologous gene expression. Values are means  $\pm$  S.D. from 4 replicate cultures (except for the glucose-grown samples, and line 6, where  $n = 3$ ). WW, wet weight; BE, branching enzyme; DBE, debranching enzyme; AGPase, ADPglucose pyrophosphorylase. (C) Light micrographs (LM) from cells of the indicated yeast lines grown as in **B**. Cells were stained with iodine. (D) Transmission electron micrographs (TEM) of the indicated yeast lines (grown as in **B**) after chemical fixation. While only particulate, putatively soluble glucans (s) were observed in line 28, line 29 also contained uniform, putatively insoluble glucans (i).

DOI: [10.7554/eLife.15552.008](https://doi.org/10.7554/eLife.15552.008)

The following source data is available for figure 3:

**Source data 1.** Glucan contents of individual replicates from strains 0 to 29.

DOI: [10.7554/eLife.15552.009](https://doi.org/10.7554/eLife.15552.009)



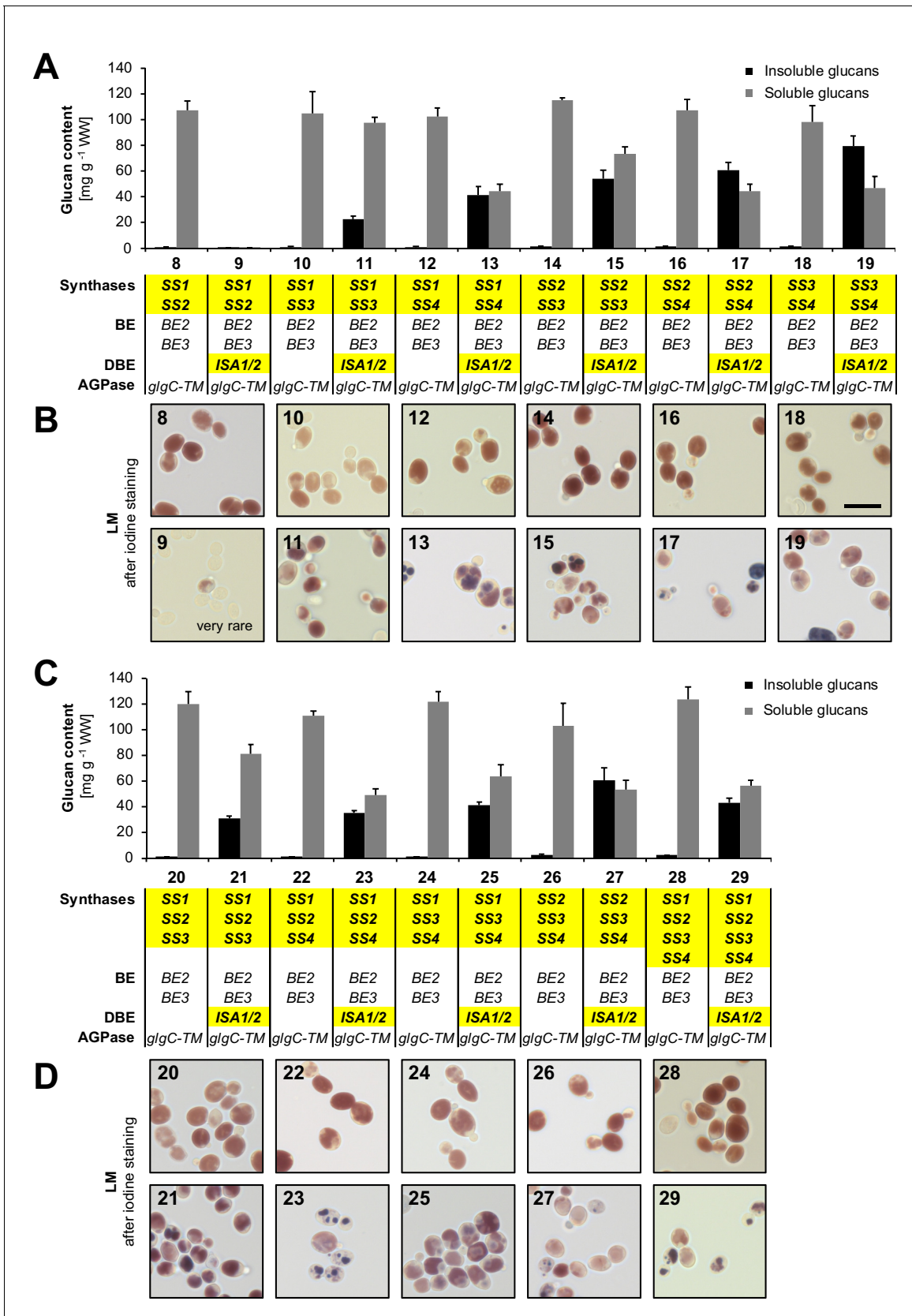


**Figure 3—figure supplement 1.** Quantification of glucans and light micrographs of yeast strains 8 to 29. (A, C) Quantification of insoluble and soluble glucans produced in the indicated yeast strains. Growth of yeast and fractionation of glucans was performed as described in **Figure 3B**. Values are **Figure 3—figure supplement 1** continued on next page

*Figure 3—figure supplement 1 continued*

means  $\pm$  S.D. from 4 replicate cultures. The data for lines 28 and 29 are the same as presented in **Figure 3B** (all yeast strains shown here and in **Figure 3B** were grown and analyzed together) and can be found in **Figure 3—source data 1**. WW, wet weight; BE, branching enzyme; DBE, debranching enzyme; AGPase, ADPglucose pyrophosphorylase. (**B, D**) Light micrographs (LM) of cells from **A** and **C**, respectively, after staining with iodine. Cells with iodine-stained glucans were obtained only rarely in line 9. The scale bar (10  $\mu$ m) applies to all pictures. Source data: **Figure 3—source data 1**. Glucan contents of individual replicates from strains 0 to 29.

DOI: [10.7554/eLife.15552.010](https://doi.org/10.7554/eLife.15552.010)

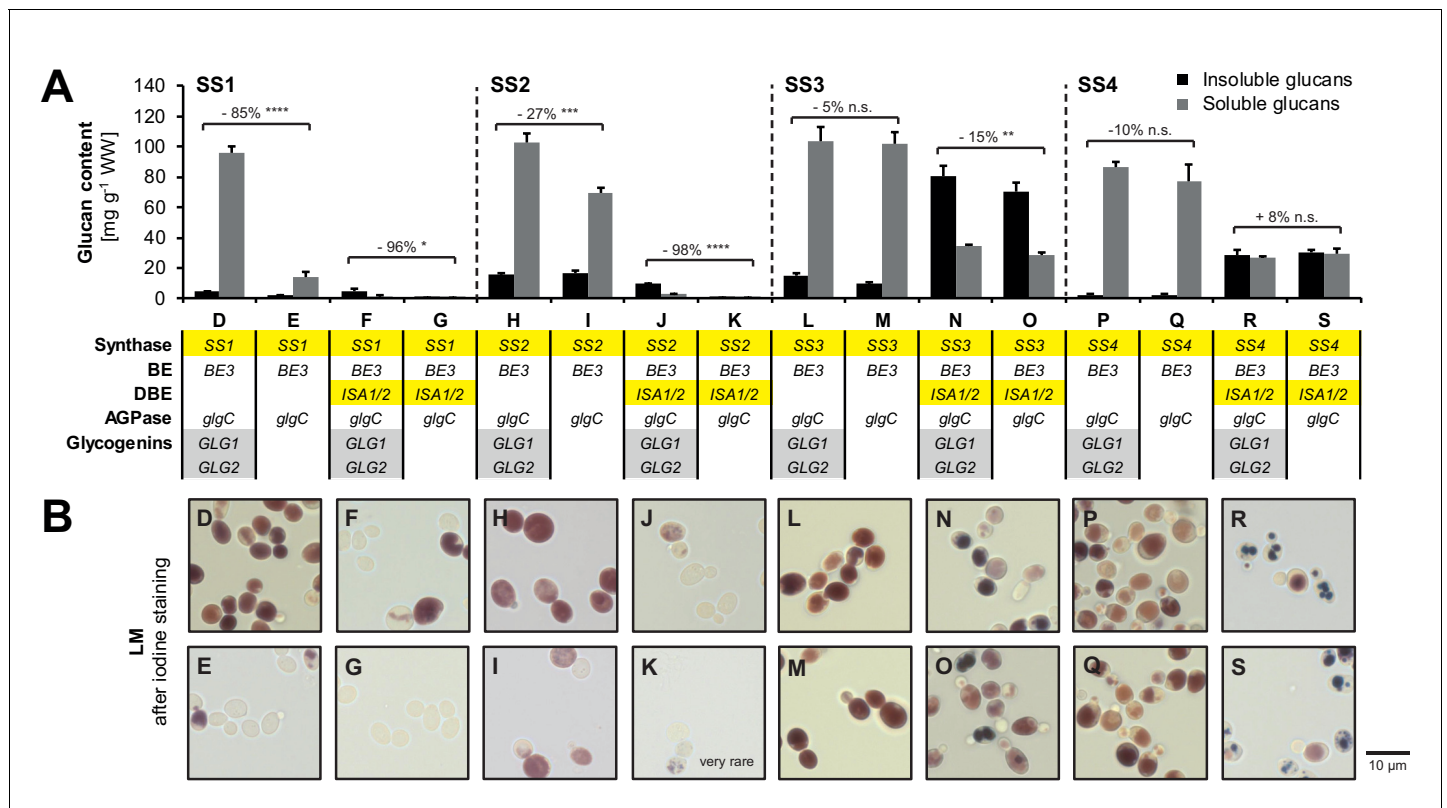


**Figure 3—figure supplement 2.** Dependence of starch synthases on glycogenins. (A) Quantification of insoluble and methanol-precipitable soluble glucans produced in the indicated yeast strains (grown as described in **Figure 3B**). The relevant genotypes are indicated; the varying Arabidopsis genes are highlighted in yellow and the endogenous yeast genes in grey. Genotypes are listed in **Supplementary file 1A**. Values are means  $\pm$  S.D. from 4 replicate cultures. Numbers indicate the percentage of change in glucan content (sum of insoluble and methanol-precipitable soluble glucans) upon loss of glycogenins. Statistical comparisons were performed using two-sided *t*-tests as described in Materials and methods. \*\*\*\**p* value < 0.0001; \*\*\**p* value < 0.001; \*\**p* value < 0.01; \**p* value < 0.05; n.s., not significant, *p* value  $\geq$  0.05. WW, wet weight; BE, branching enzyme; DBE, debranching enzyme; AGPase, ADPglucose pyrophosphorylase. (B) Light micrographs of cells from **A** after staining with iodine. Cells with iodine-stained glucans were obtained only rarely in line K. In case of SS1, deletion of both endogenous glycogenins *GLG1* and *GLG2* resulted in a marked reduction in glucan content with only few (strain E) or no (strain G) cells remaining capable of glucan production. This effect was additive to that of *ISA1/ISA2* expression (which also repeatedly reduced glucan accumulation in yeasts where only SS1 and/or SS2 were present). Strains with SS2 produced fewer glucans when glycogenins were absent, but the difference was small when *ISA* was absent. SS3 showed no or little dependence on glycogenins and no dependence was observed in case of SS4.

DOI: 10.7554/eLife.15552.011

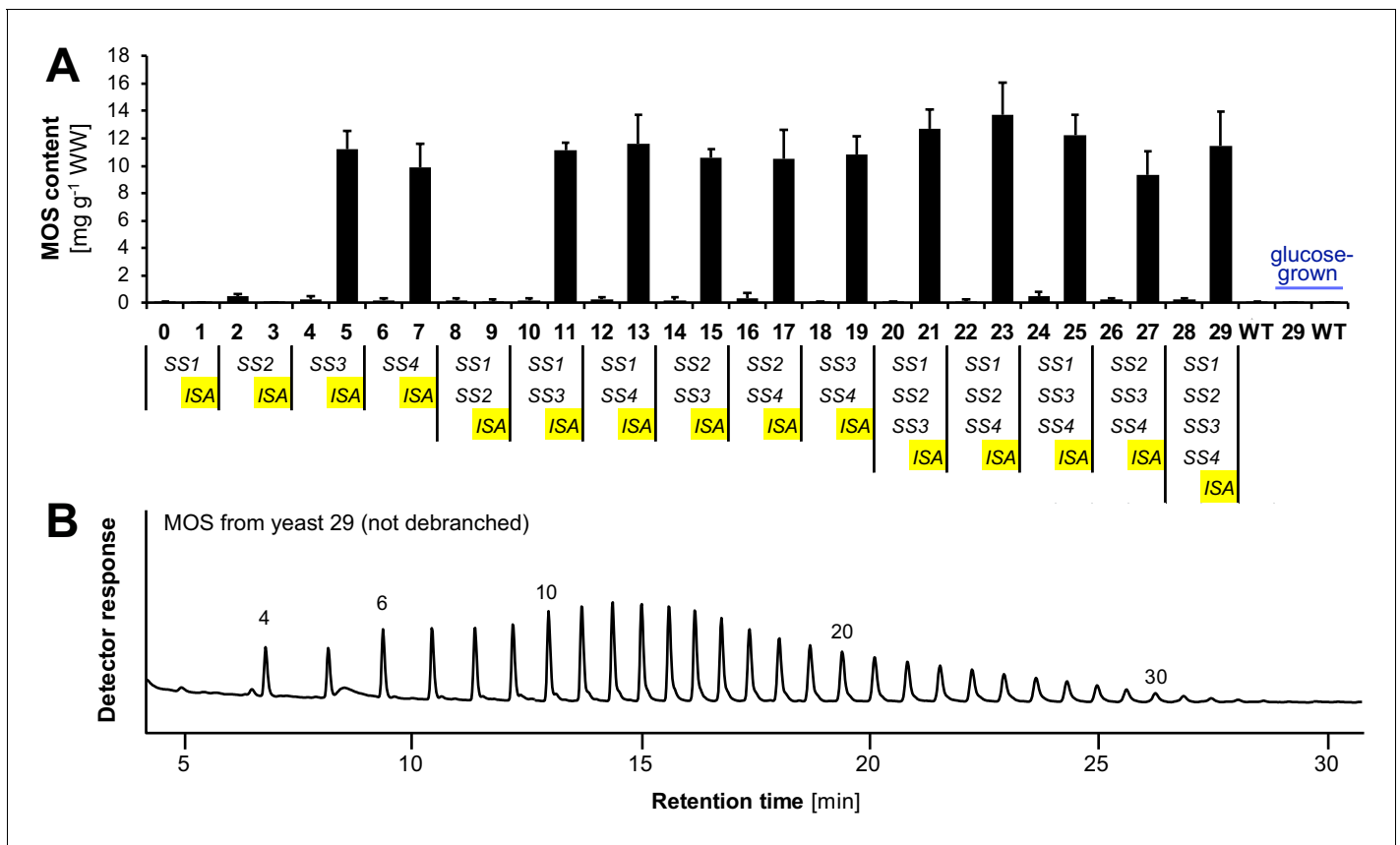


**Figure 3—figure supplement 3.** Accumulation of linear malto-oligosaccharides (MOS) in the presence of isoamylase. (A) Quantification of malto-oligosaccharides (MOS) of the yeast samples presented in **Figure 3B** and **Figure 3—figure supplement 1**. All lines also contain *BE2*, *BE3* and *glgC-TM*. Values are means  $\pm$  S.D. from 4 replicate cultures (except for the glucose-grown samples and line 6, where  $n = 3$ ). The MOS contents of individual replicates can be found in **Figure 3—source data 1**. (B) Chain-length distribution of malto-oligosaccharides from line 29 that were not enzymatically debranched during sample preparation. Numbers indicate the degree of polymerization (DP) of the corresponding linear chains. Branched chains typically elute slightly earlier than linear chains of the same molecular weight and were absent in the chromatograms. A representative chromatogram from one replicate culture is shown. Similar results were obtained in a second replicate from line 29 and for malto-oligosaccharides from the three other lines tested (lines 7, 11, and 17). Source data: **Figure 3—source data 1**. Glucan contents of individual replicates from strains 0 to 29.

DOI: [10.7554/eLife.15552.012](https://doi.org/10.7554/eLife.15552.012)

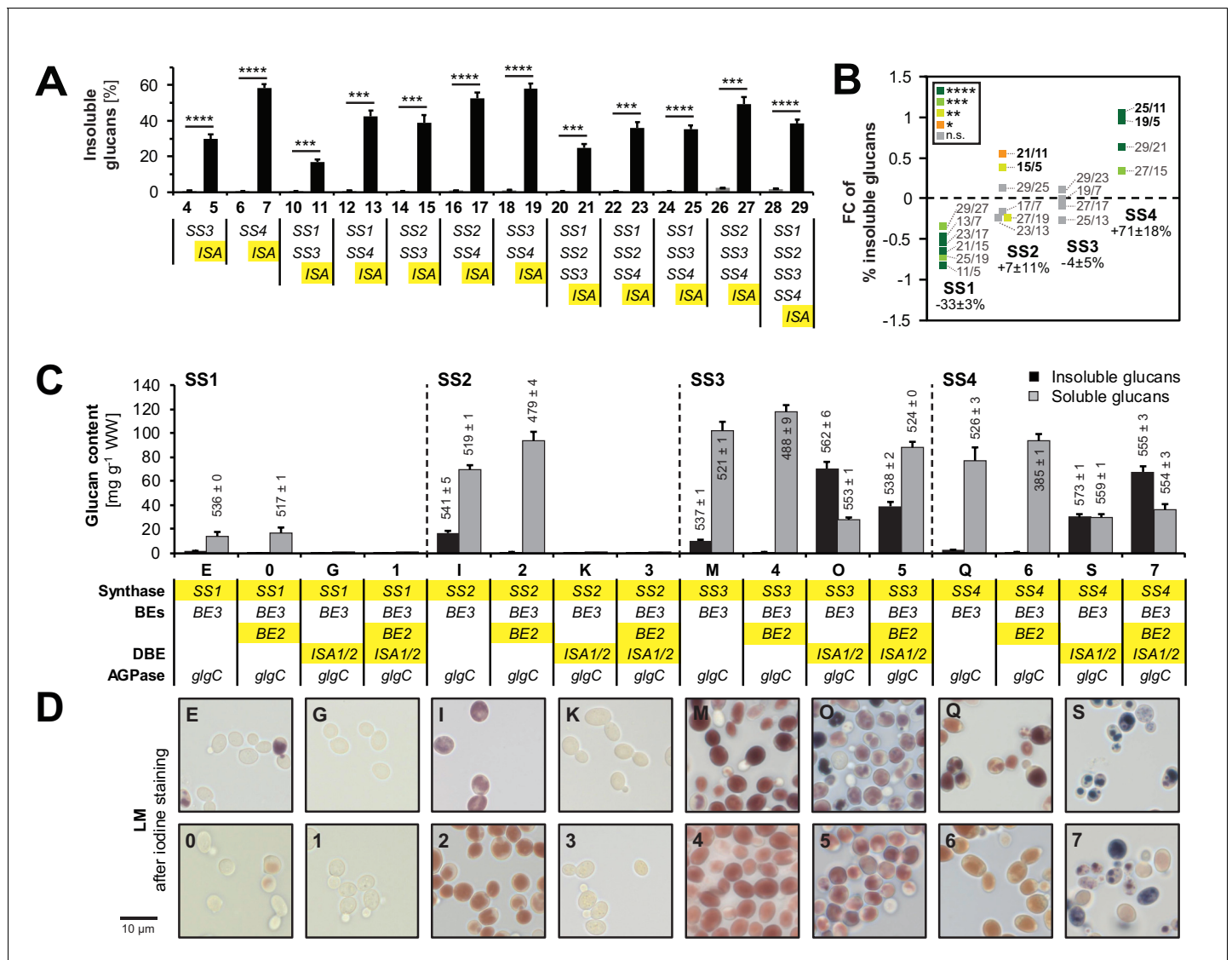


**Figure 4.** Isoamylase, starch synthases and branching enzymes have distinct effects on the formation of insoluble glucans. (A) Percentage of total glucans that were insoluble glucans of lines without isoamylase (grey bars) and their corresponding partners with isoamylase (ISA, black bars). Only strain pairs in which both lines have glucan levels > 5 mg g<sup>-1</sup> wet weight (WW) were included. All lines furthermore contain BE2, BE3 and *glgC-TM*. Values are means ± S.D. from 4 replicate cultures, except for line 6 (n = 3). Statistical comparisons were performed using two-sided t-tests as described in Materials and methods. The underlying data is available in **Figure 3—source data 1**. \*\*\*\*p value < 0.0001; \*\*\*p value < 0.001. (B) Fold changes (FC) of percentage of insoluble glucans depending on individual SS, using data from lines with ISA presented in A. The compared lines are indicated. The comparisons of SS2 in the absence of SS4 and vice versa are shown in bold. Given values for each SS are mean percentage changes from all comparisons ± S.E.M. (n = 6 for SS1 and SS2, n = 4 for SS3 and SS4; see **Figure 4—source data 1** for the calculations). Statistical comparisons were performed using ANOVA as described in Materials and methods. \*\*\*\*p value < 0.0001; \*\*\*p value < 0.001; \*\*p value < 0.01; \*p value < 0.05; n.s., not significant, p value ≥ 0.05. (C) Quantification of insoluble (black bars) and methanol-precipitable soluble (grey bars) glucans and their wavelengths of maximum absorption after complexation with iodine (λ<sub>max</sub>, values above/below the bars, in nm). Yeast lines were grown as described in **Figure 3B**. Values are means ± S.D. from 4 replicate cultures for quantifications and from 2 replicate cultures for the λ<sub>max</sub> measurements (except for insoluble glucans from strains I, 5 and 7 where n = 4). The quantification data for lines E, G, I, K, M, O, Q and S are the same as presented in **Figure 3—figure supplement 2** (all yeast strains shown here and in **Figure 3—figure supplement 2** were grown and analyzed together). WW, wet weight; BEs, branching enzymes; DBE, debranching enzyme; AGPase, ADPglucose pyrophosphorylase. (D) Light micrographs of cells from A after staining with iodine. Bar = 10 μm. Source data: DOI: 10.7554/eLife.15552.013

The following source data is available for figure 4:

**Source data 2.** Glucan contents and λ<sub>max</sub> values of individual replicates.

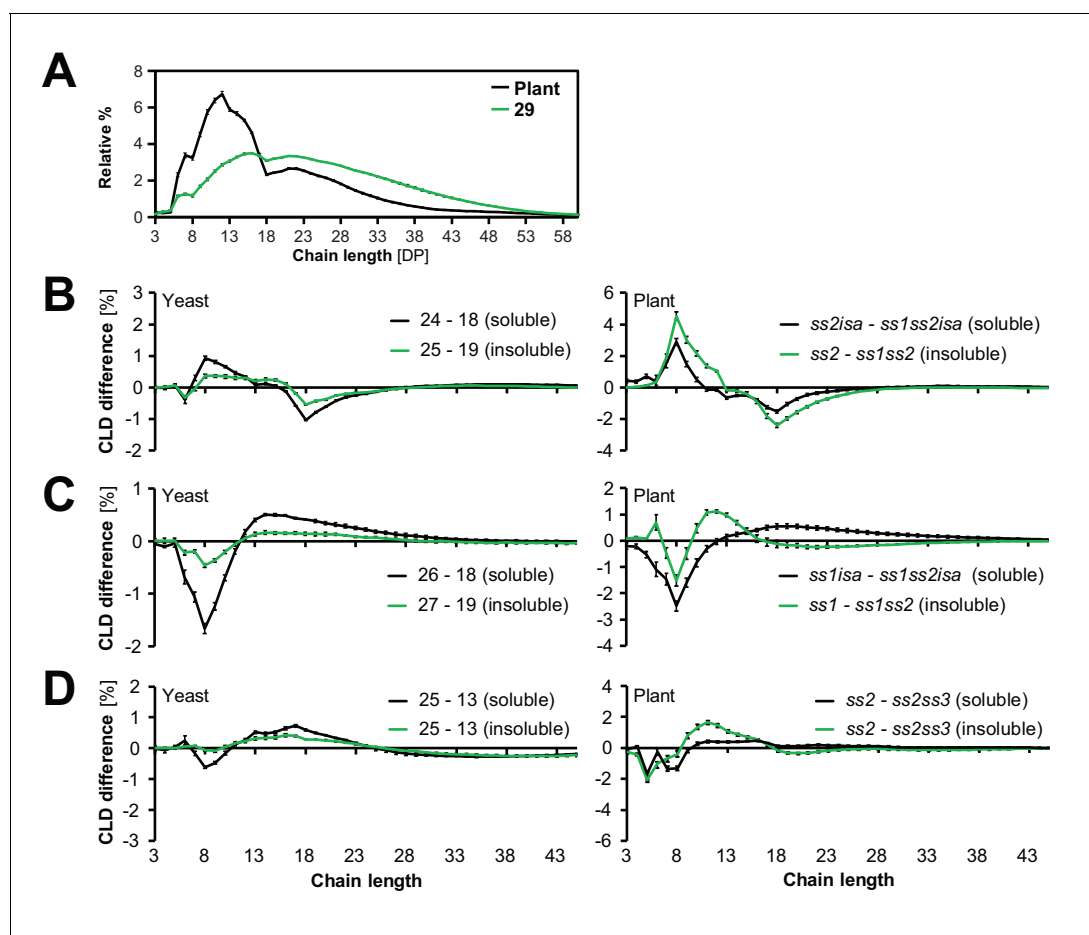
DOI: 10.7554/eLife.15552.014

Figure 4 continued on next page

Figure 4 continued

**Source data 1.** Glucan contents of individual replicates from strains 0 to 29.

DOI: [10.7554/eLife.15552.015](https://doi.org/10.7554/eLife.15552.015)



**Figure 5.** Starch synthases retain their chain-elongation specificities. (A) Chain length distributions (CLDs) of debranched insoluble glucans from line 29 and of wild-type Arabidopsis starch (WS ecotype). Values are means  $\pm$  S.D. from 4 replicate yeast cultures or 3 plants, respectively. The CLD of *gbss* mutant Arabidopsis starch is reported to be identical to that from wild-type starch (Seung et al., 2015). (B-D) Representative graphs illustrating the changes in glucan fine structure upon the addition of SS1 (B), SS2 (C) or SS3 (D) in yeast and *in planta*. Comparisons were done by subtracting the CLDs as indicated (means  $\pm$  S.E.M.,  $n = 4$ , except for *ss2isa*, *ss1isa*, *ss2*, yeast line 13 (soluble) and *ss2* [insoluble shown in B and D], where  $n = 3$ ). Data from plants in B and C are recalculations from Pfister et al., (2014). Horizontal comparisons in yeast and *in planta* involve the same set of amylopectin-synthesizing genes in each case (i.e. line 24 has the whole known complement except for SS2 and ISA1/ISA2, corresponding to an *ss2isa* mutant; line 18 the same enzymes except for SS1, corresponding to an *ss1ss2isa* mutant). Subtracting the CLD of line 18 from that of line 24 thus reveals the effect of the presence of SS1.

DOI: 10.7554/eLife.15552.016

The following source data is available for figure 5:

**Source data 1.** Numerical data of chain-length distributions from the plant and yeast glucans.

DOI: 10.7554/eLife.15552.017

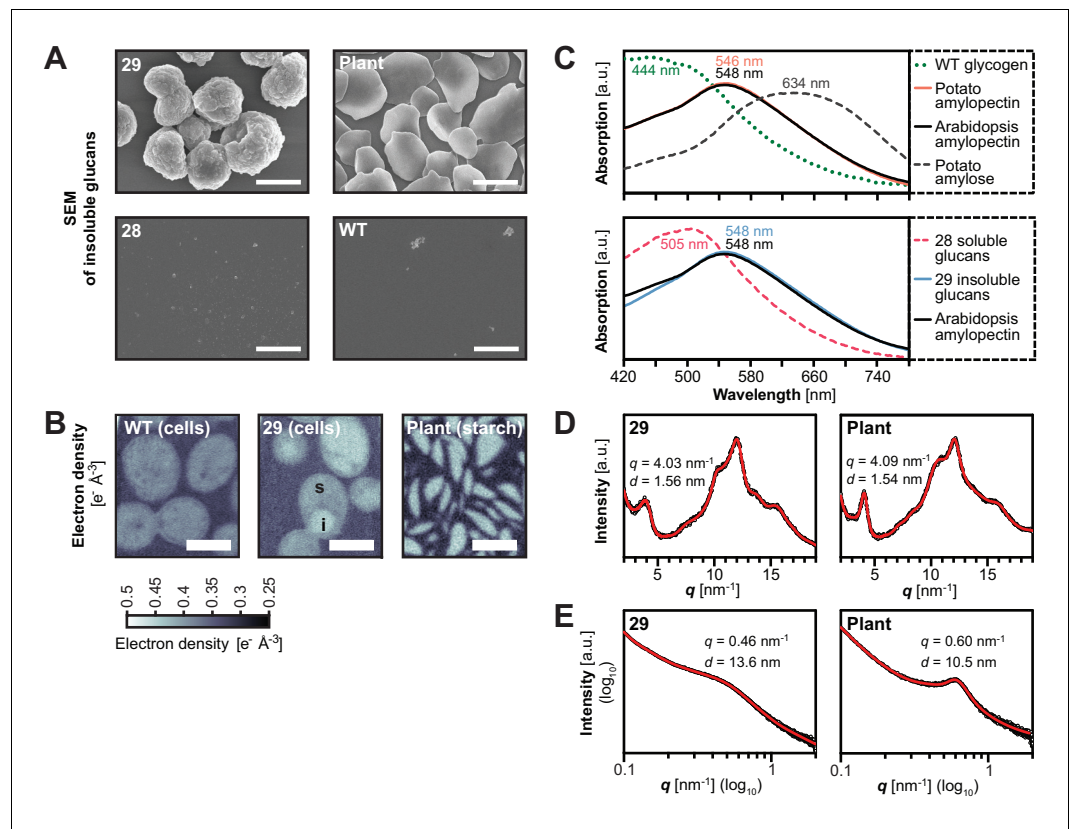


**Figure 6.** Structure of starch granules made in *S.cerevisiae* compared with amylose-free Arabidopsis starch. (A) Scanning electron micrographs (SEMs) of purified insoluble particles from line 29 and of amylose-free Arabidopsis starch. No insoluble particles could be purified from WT yeast or line 28. The granules of WT Arabidopsis starch are similar to those of amylose-free starch (Figure 6—figure supplement 1). Bars = 2  $\mu\text{m}$ . (B) 2D slices through 3D electron density maps obtained by cryo X-ray ptychographic tomography of intact yeast cells (grown as in Figure 3B) and purified amylose-free Arabidopsis starch granules. i, putative insoluble glucans; s, putative soluble glucans; bars = 3  $\mu\text{m}$ . (C) Absorption spectra of glucans from the indicated yeast lines (WT, line 28 and line 29) and various plant glucans after complexation with iodine. Wavelengths of maximum absorption are indicated. a.u., arbitrary units. (D) Wide-angle and (E) small-angle X-ray scattering intensity profiles of insoluble glucans from line 29 and amylose-free Arabidopsis starch (i.e. amylopectin). The profiles of WT Arabidopsis starch are similar to those of amylose-free starch (Figure 6—figure supplement 3).  $q$ , scattering vector;  $d$ , lamellar periodicity; a.u., arbitrary units. The following figure supplements are available for Figure 6:

DOI: [10.7554/eLife.15552.018](https://doi.org/10.7554/eLife.15552.018)



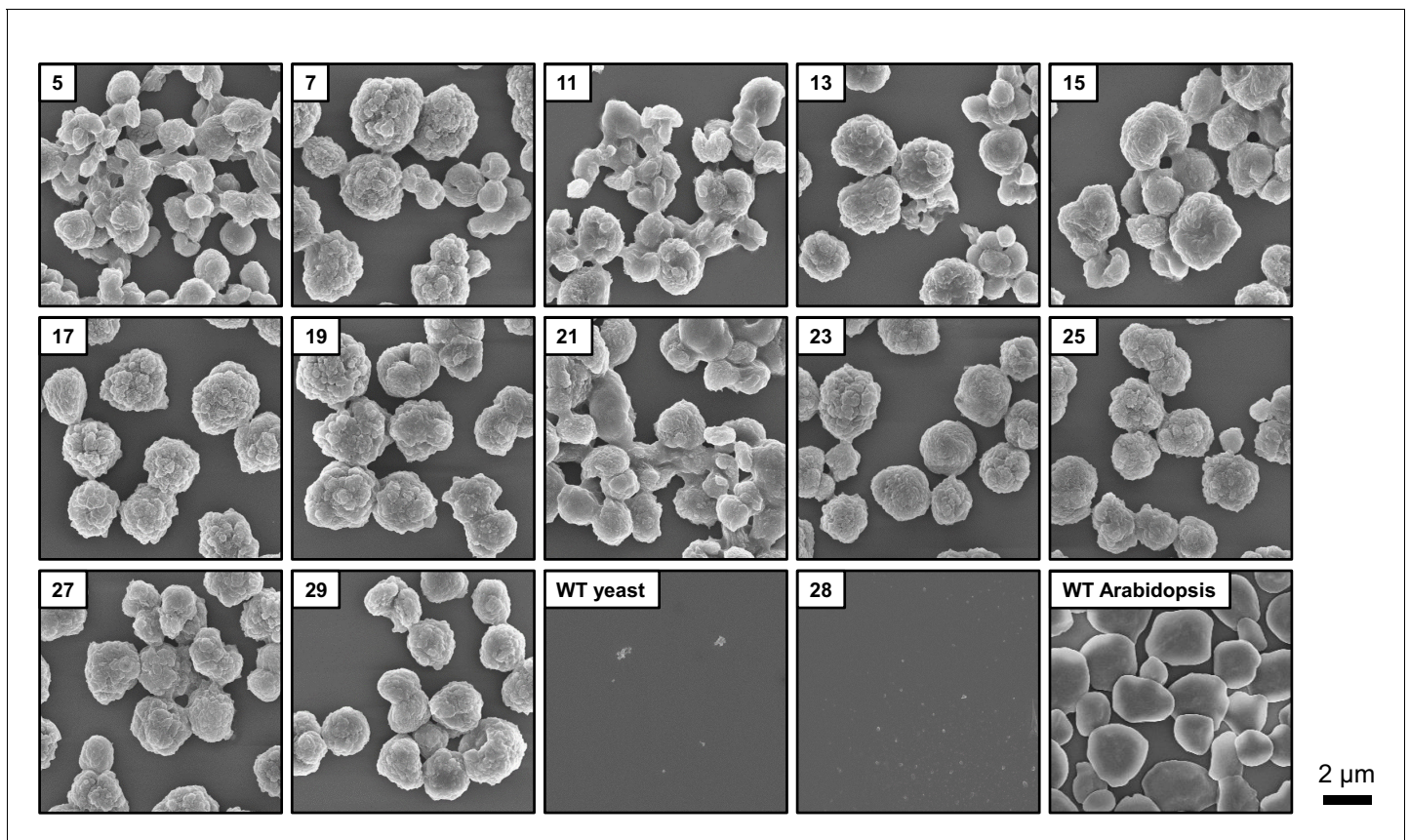


**Figure 6—figure supplement 1.** Scanning electron micrographs (SEMs) of purified insoluble particles from the indicated yeast strains and from wild-type Arabidopsis (WS ecotype) leaf starch. The micrographs from lines 28, 29 and WT yeast are the same as shown in **Figure 5A**.

DOI: [10.7554/eLife.15552.019](https://doi.org/10.7554/eLife.15552.019)

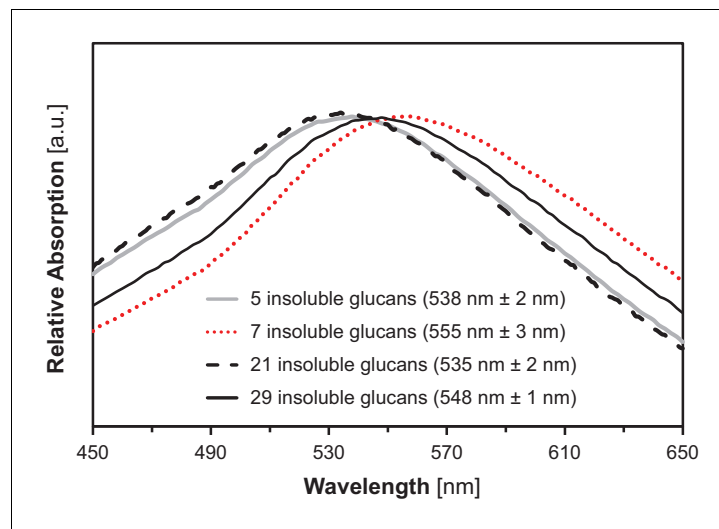


**Figure 6—figure supplement 2.** Absorption spectra of insoluble glucans from the indicated yeast lines. Shown is one representative spectrum from one replicate. Wavelengths of maximum absorption (means  $\pm$  S.D. from 4 biological replicates) are indicated in brackets. a.u., arbitrary units.

DOI: [10.7554/eLife.15552.020](https://doi.org/10.7554/eLife.15552.020)

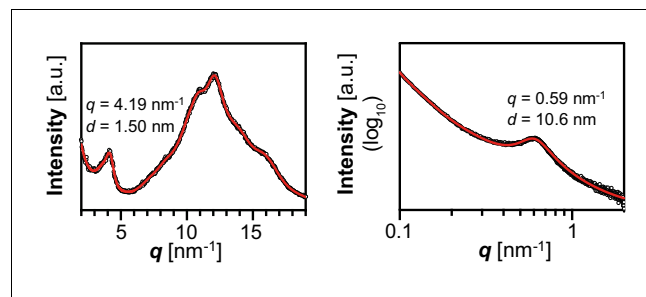


**Figure 6—figure supplement 3.** X-ray scattering wild-type Arabidopsis starch. Wide-angle (left) and small-angle (right) X-ray scattering intensity profiles of purified WT Arabidopsis starch (Col-0 ecotype).  $q$ , scattering vector;  $d$ , lamellar periodicity; a.u., arbitrary units.

DOI: [10.7554/eLife.15552.021](https://doi.org/10.7554/eLife.15552.021)